Constraints on models for the Higgs boson with exotic spin and parity in $VH \to Vb\bar{b}$ final states

(The D0 Collaboration)

(Dated: August 28, 2014)

SUPPLEMENTAL MATERIAL

In this document we provide supplemental information on the constraints on models with non-SM spin and parity for the Higgs boson in the $VH \to Vb\bar{b}$ final states in up to 9.7 fb^{-1} of $p\bar{p}$ collisions at $\sqrt{s} = 1.96$ TeV collected with the D0 detector at the Fermilab Tevatron Collider. We denote a non-SM Higgs boson as X.

Figure 1: Dijet mass distributions for the $\nu\nu b\bar{b}$ and $\ell\ell b\bar{b}$ analyses and the BDT output distribution for the $\ell\nu b\bar{b}$ analysis.

Figures 2–5: Additional VX invariant and transverse mass distributions for individual analyses.

Figures 6 and 7: LLR distributions for the individual analyses and their combination.

Tables I and II: Tables of CL_{H_x} and $1 - CL_s$ values for the individual analyses and their combination for $\mu = 1.0$ and $\mu = 1.23$.

Figure 8: $1 - CL_s$ as a function of the $J^P = 2^+$ signal fraction, f_{2^+}, for all analyses combined.

Figure 9: The expected and observed 95% CL exclusion as functions of the $J^P = 0^-$ ($J^P = 2^+$) signal fraction, f_{0^-} (f_{2^+}), and the total signal strength.

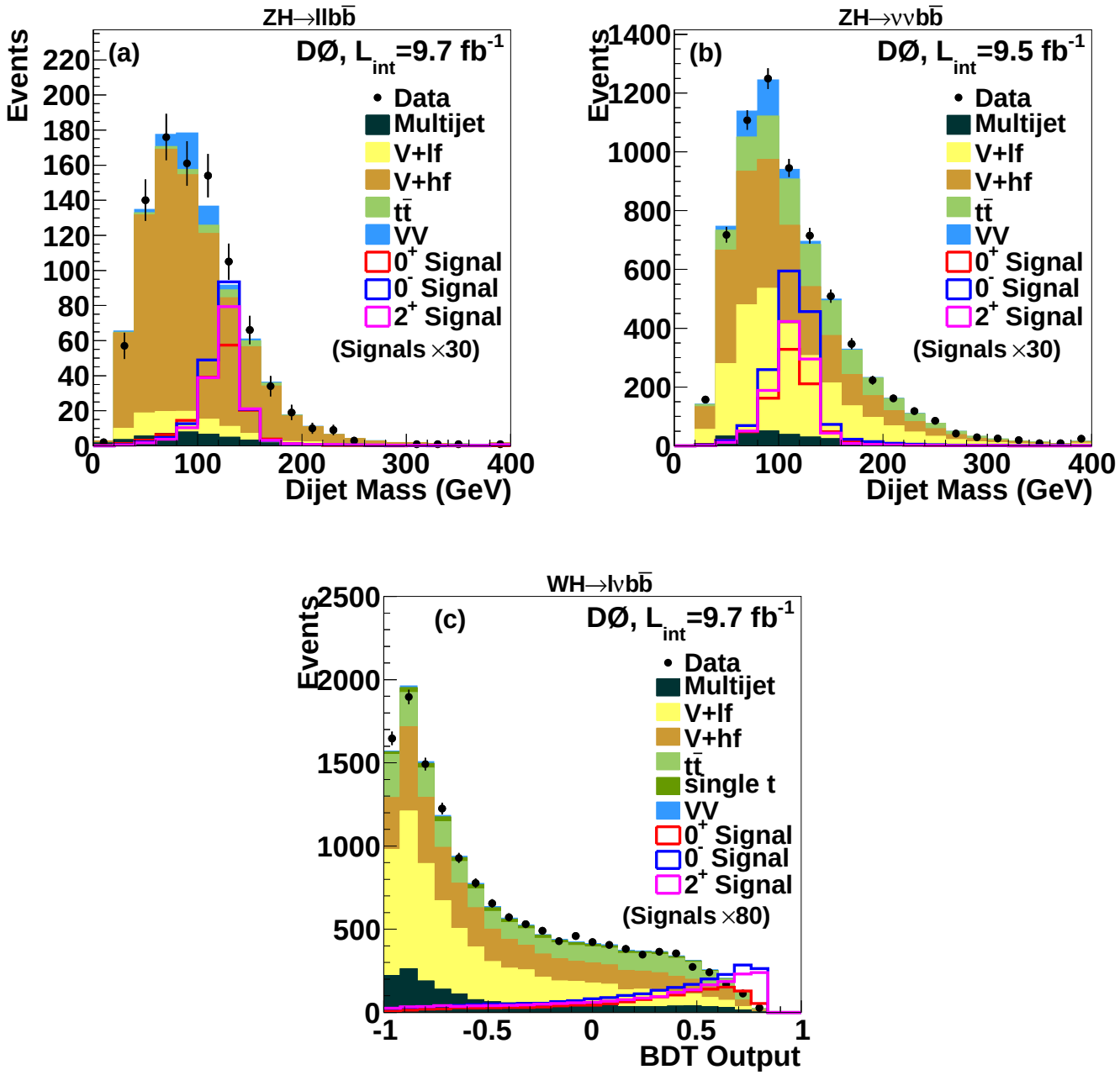

FIG. 1: Invariant mass of the dijet system for (a) the $ZH \to \ell\ell b\bar{b}$ analysis, and (b) the $ZH \to \nu\nu b\bar{b}$ analysis, and the BDT output for (c) the $WH \to \ell\nu b\bar{b}$ analysis. The $J^P = 2^+$ and $J^P = 0^-$ samples are normalized to the product of the SM cross section and branching fraction multiplied by an additional factor. Heavy- and light-flavor quark jets are denoted by lf and hf, respectively. Overflow events are included in the highest bin. For all signals, a mass of 125 GeV for the H or X boson is assumed.

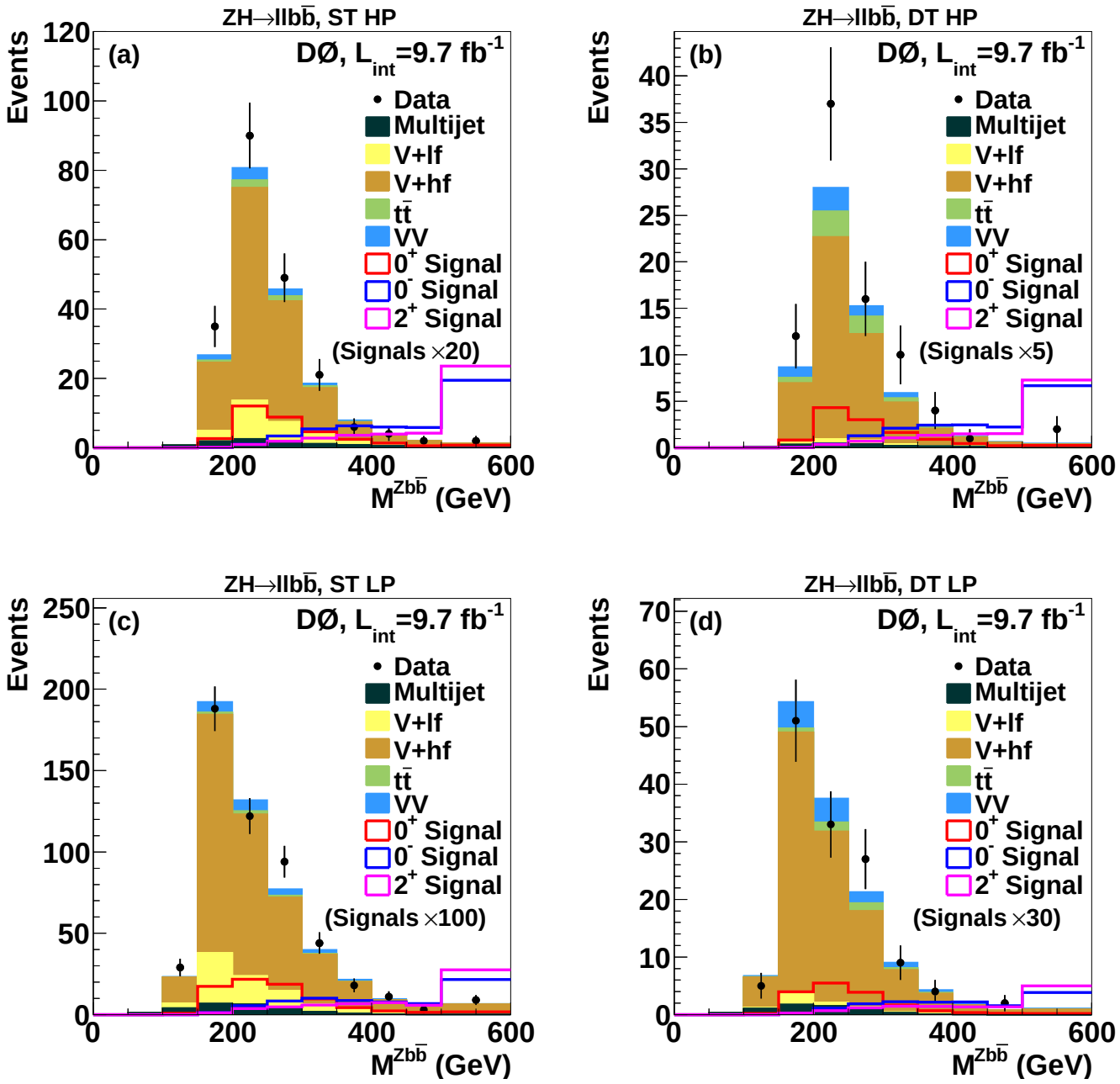

FIG. 2: Invariant mass of the $\ell\ell b\bar{b}$ system in the $ZH \to \ell\ell b\bar{b}$ analysis for events in the (a) single-tag high-purity (ST HP), (b) double-tag high-purity (DT HP), (c) single-tag low-purity (ST LP), and (d) double-tag low-purity (DT LP) channels. The $J^P = 2^+$ and $J^P = 0^-$ samples are normalized to the product of the SM cross section and branching fraction multiplied by an additional factor. Heavy- and light-flavor quark jets are denoted by lf and hf, respectively. Overflow events are included in the last bin. For all signals, a mass of 125 GeV for the H or X boson is assumed.

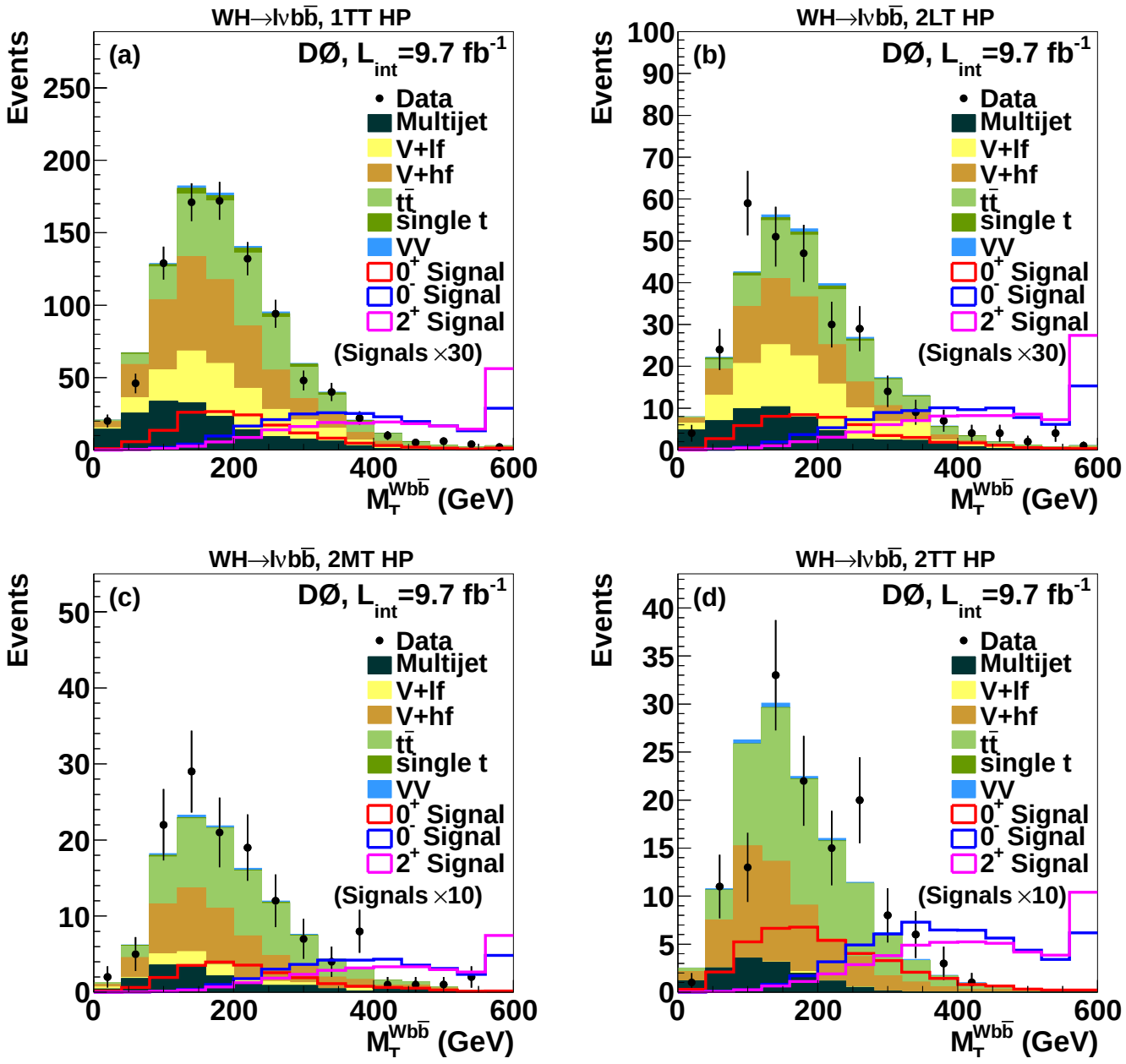

FIG. 3: Transverse mass of the $\ell\nu b\bar{b}$ system in the $WH \to \ell\nu b\bar{b}$ analysis in the high-purity (HP) region for (a) 1 tight-tag (1TT), (b) 2 loose-tags (2LT), (c) 2 medium-tags (2MT), and (d) 2 tight-tags (2TT) channels. The $J^P = 2^+$ and $J^P = 0^-$ samples are normalized to the product of the SM cross section and branching fraction multiplied by an additional factor. Heavy- and light-flavor quark jets are denoted by lf and hf, respectively. Overflow events are included in the last bin. For all signals, a mass of 125 GeV for the H or X boson is assumed.

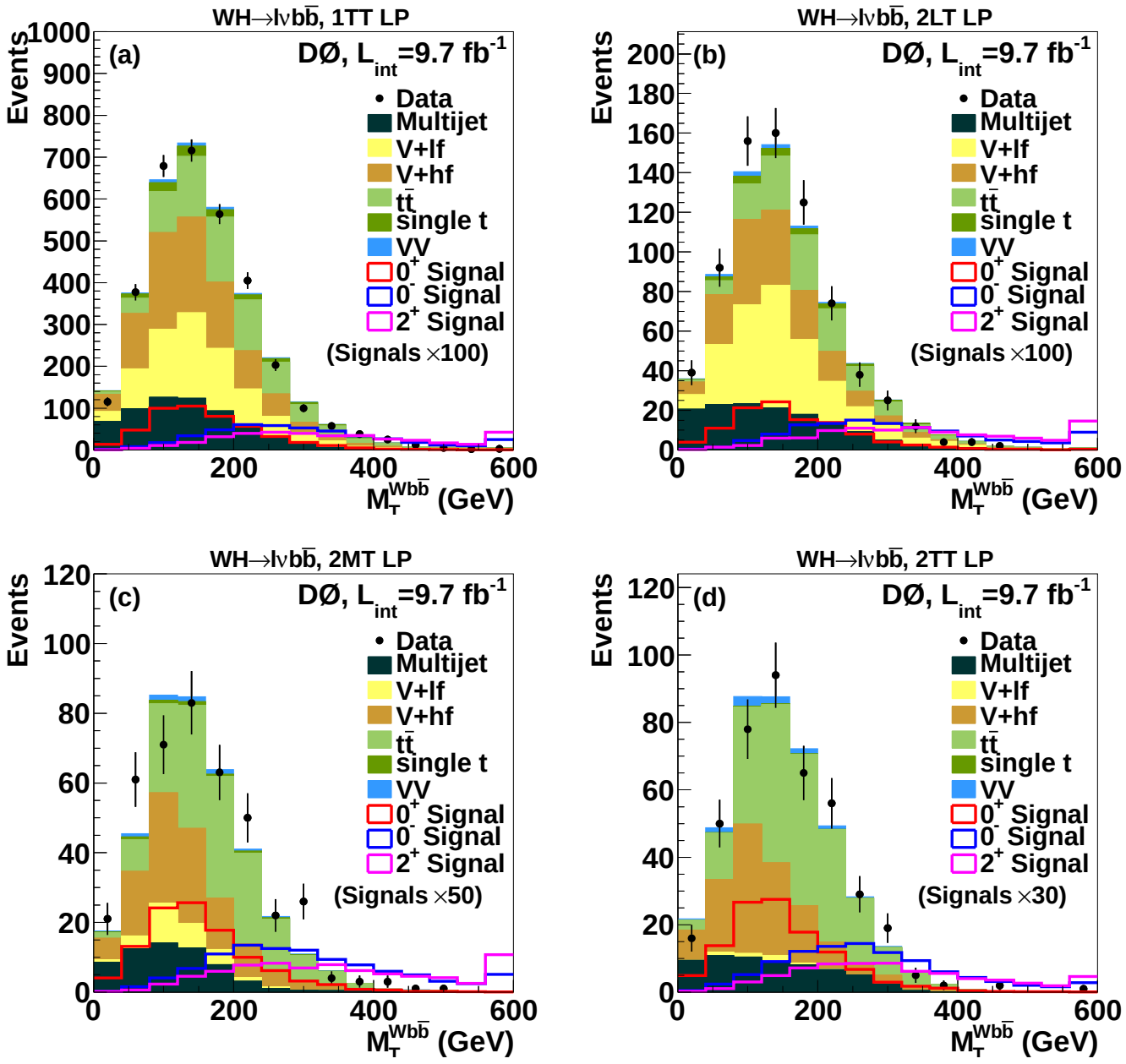

FIG. 4: Transverse mass of the $\ell\nu b\bar{b}$ system in the $WH \to \ell\nu b\bar{b}$ analysis in the low purity (LP) region for (a) 1-tight-tag (1TT), (b) 2-loose-tags (2LT), (c) 2-medium-tags (2MT), and (d) 2-tight-tags (2TT) channels. The $J^P = 2^+$ and $J^P = 0^-$ samples are normalized to the product of the SM cross section and branching fraction multiplied by an additional factor. Heavy- and light-flavor quark jets are denoted by lf and hf, respectively. Overflow events are included in the last bin. For all signals, a mass of 125 GeV for the H or X boson is assumed.

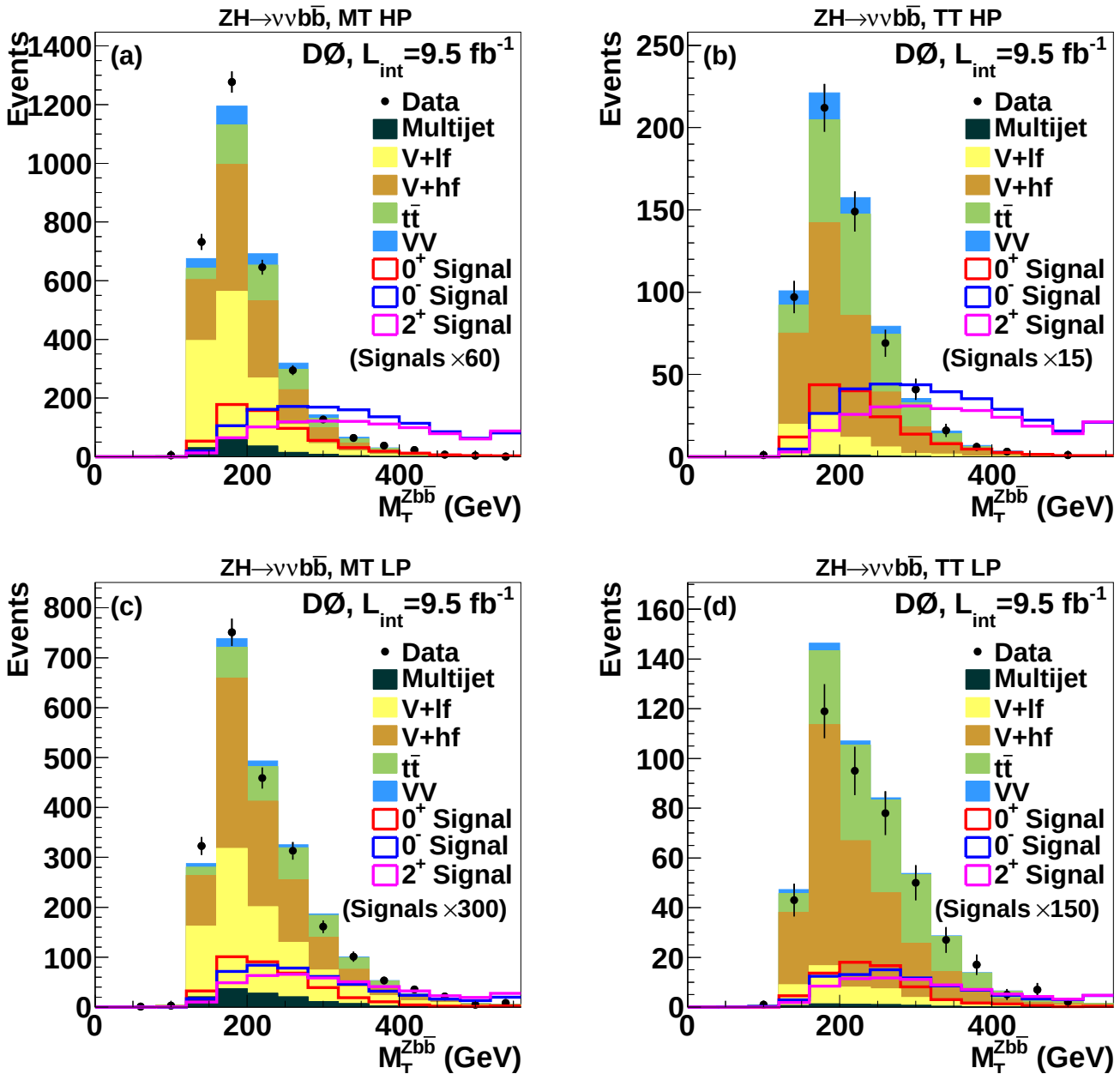

FIG. 5: Transverse mass of the $\nu\nu b\bar{b}$ system in the $ZH \to \nu\nu b\bar{b}$ analysis for events in the (a) medium-tag high-purity (MT HP), (b) tight-tag high-purity (TT HP), (c) medium-tag low-purity (MT LP), and (d) tight-tag low-purity (TT LP) channels. The $J^P = 2^+$ and $J^P = 0^-$ samples are normalized to the product of the SM cross section and branching fraction multiplied by an additional factor. Heavy- and light-flavor quark jets are denoted by lf and hf, respectively. Overflow events are included in the last bin. For all signals, a mass of 125 GeV for the H or X boson is assumed.

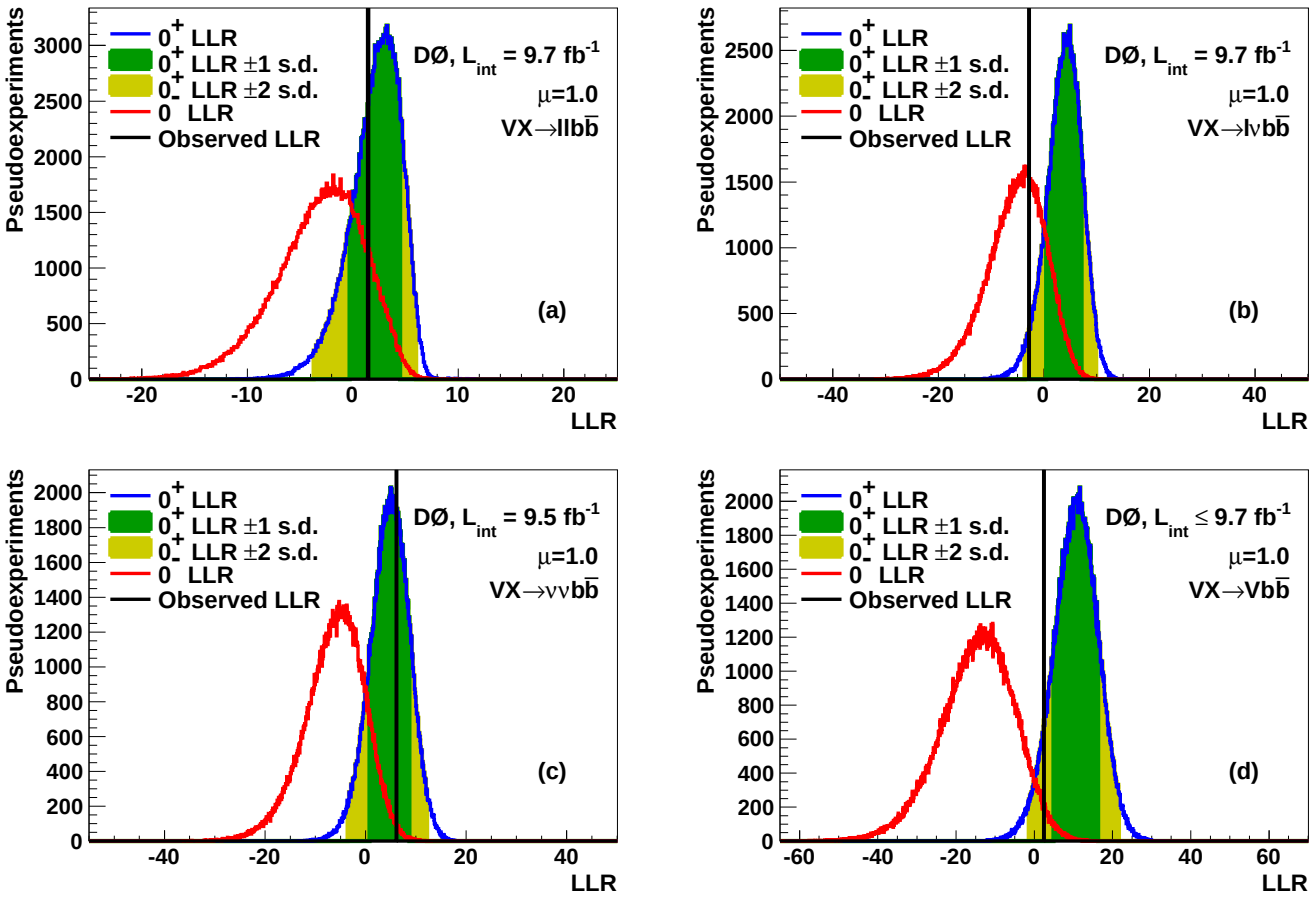

FIG. 6: LLR distributions comparing the $J^P = 0^+$ and the $J^P = 0^-$ hypotheses for the (a) $ZH \to \ell\ell b\bar{b}$ analysis, (b) $WH \to \ell\nu b\bar{b}$ analysis, (c) $ZH \to \nu\nu b\bar{b}$ analysis, and (d) their combination. The $J^P = 0^+$ and $J^P = 0^-$ samples are normalized to the product of the SM cross section and branching fraction multiplied by $\mu = 1.0$. The vertical solid line represents the observed LLR value, while the dark and light shaded areas represent 1 s.d. and 2 s.d. on the expectation from the null hypothesis H_0, respectively. Here H_0 is the SM $J^P = 0^+$ signal plus backgrounds. For all signals, a mass of 125 GeV for the H or X boson is assumed.

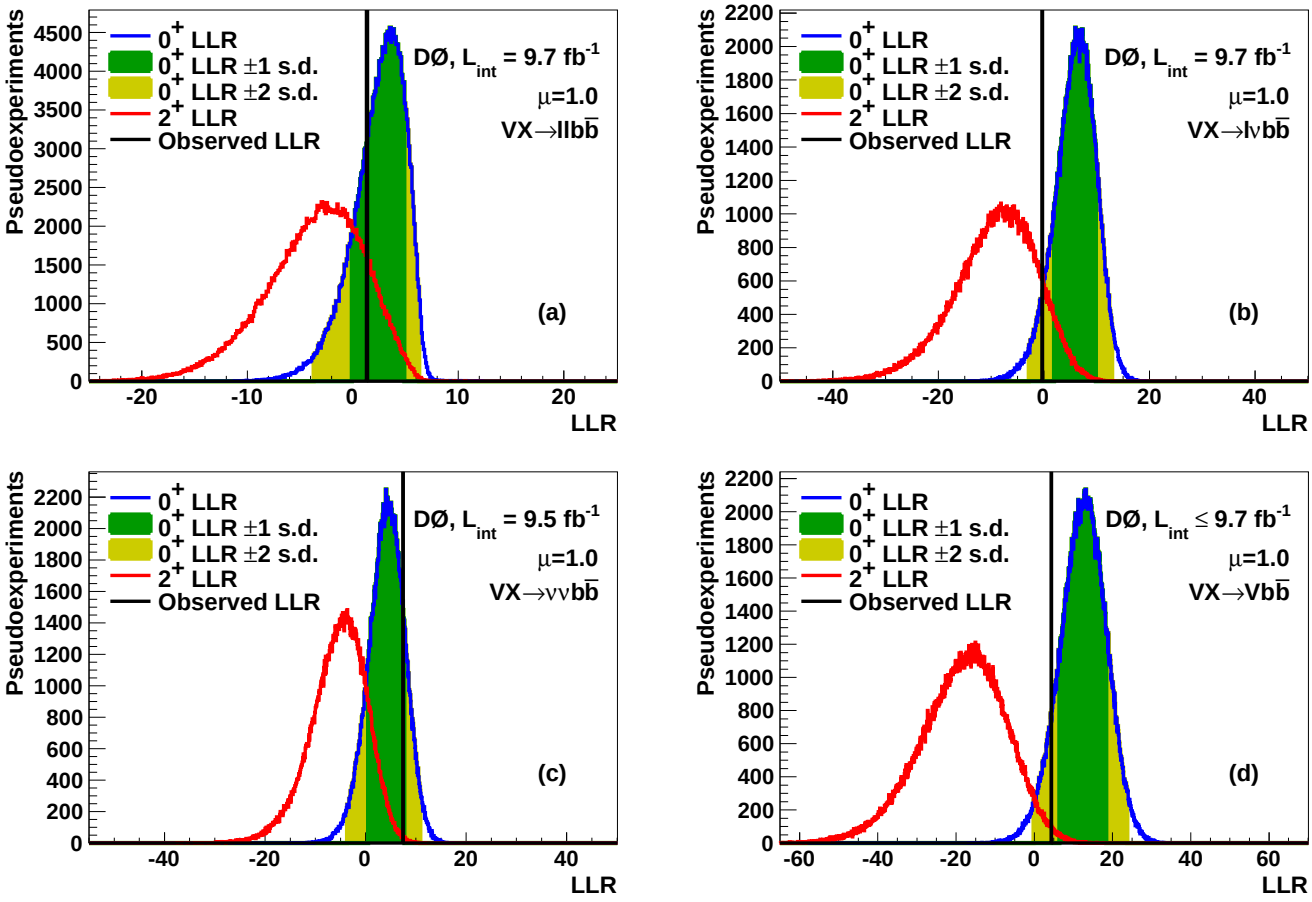

FIG. 7: LLR distributions comparing the $J^P = 0^+$ and the $J^P = 2^+$ hypotheses for the (a) $ZH \to \ell\ell b\bar{b}$ analysis, (b) $WH \to \ell\nu b\bar{b}$ analysis, (c) $ZH \to \nu\nu b\bar{b}$ analysis, and (d) their combination. The $J^P = 0^+$ and $J^P = 2^+$ samples are normalized to the product of the SM cross section and branching fraction multiplied by $\mu = 1.0$. The vertical solid line represents the observed LLR value, while the dark and light shaded areas represent 1 s.d. and 2 s.d. on the expectation from the null hypothesis H_0, respectively. Here H_0 is the SM $J^P = 0^+$ signal plus backgrounds. For all signals, a mass of 125 GeV for the H or X boson is assumed.

Analysis	$ZH \to \ell\ell b\bar{b}$	$WH \to \ell\nu b\bar{b}$	$ZH \to \nu\nu b\bar{b}$	Combined
	$J^P = 0^-$ vs. $J^P = 0^+$			
CL_{0^-} Expected	0.075	0.030	0.016	0.0007
CL_{0^-} Observed	0.126	0.351	0.007	0.022
CL_{0^+} Expected	0.500	0.500	0.500	0.500
CL_{0^+} Observed	0.646	0.965	0.367	0.918
$1 - CL_s$ Expected	0.850 (1.04 s.d.)	0.941 (1.56 s.d.)	0.969 (1.87 s.d.)	0.9986 (3.00 s.d.)
$1 - CL_s$ Observed	0.805 (0.86 s.d.)	0.637 (0.35 s.d.)	0.981 (2.07 s.d.)	0.976 (1.98 s.d.)
	$J^P = 2^+$ vs. $J^P = 0^+$			
CL_{2^+} Expected	0.064	0.009	0.023	0.0003
CL_{2^+} Observed	0.134	0.114	0.002	0.009
CL_{0^+} Expected	0.500	0.500	0.500	0.500
CL_{0^+} Observed	0.702	0.932	0.173	0.906
$1 - CL_s$ Expected	0.872 (1.14 s.d.)	0.982 (2.09 s.d.)	0.953 (1.68 s.d.)	0.9994 (3.22 s.d.)
$1 - CL_s$ Observed	0.810 (0.88 s.d.)	0.878 (1.16 s.d.)	0.987 (2.23 s.d.)	0.990 (2.34 s.d.)

TABLE I: Expected and observed CL_{H_x} and $1 - CL_s$ values for $J^P = 0^-$ and $J^P = 2^+$ VX associated production, assuming signal cross sections equal to the 125 GeV SM Higgs production cross section multiplied by $\mu = 1.0$. The null hypothesis is taken to be the sum of the SM Higgs boson signal and background production.

Analysis	$ZH \to \ell\ell b\bar{b}$	$WH \to \ell\nu b\bar{b}$	$ZH \to \nu\nu b\bar{b}$	Combined
	$J^P = 0^-$ vs. $J^P = 0^+$			
CL_{0^-} Expected	0.046	0.012	0.005	<0.0001
CL_{0^-} Observed	0.072	0.245	0.0006	0.005
CL_{0^+} Expected	0.500	0.500	0.500	0.500
CL_{0^+} Observed	0.615	0.971	0.215	0.922
$1 - CL_s$ Expected	0.908 (1.33 s.d.)	0.975 (1.96 s.d.)	0.989 (2.31 s.d.)	0.9998 (3.60 s.d.)
$1 - CL_s$ Observed	0.883 (1.19 s.d.)	0.747 (0.67 s.d.)	0.997 (2.78 s.d.)	0.995 (2.56 s.d.)
	$J^P = 2^+$ vs. $J^P = 0^+$			
CL_{2^+} Expected	0.037	0.003	0.009	<0.0001
CL_{2^+} Observed	0.078	0.056	0.003	0.002
CL_{0^+} Expected	0.500	0.500	0.500	0.500
CL_{0^+} Observed	0.679	0.937	0.363	0.911
$1 - CL_s$ Expected	0.925 (1.44 s.d.)	0.995 (2.56 s.d.)	0.983 (2.11 s.d.)	0.9999 (3.86 s.d.)
$1 - CL_s$ Observed	0.885 (1.20 s.d.)	0.941 (1.56 s.d.)	0.991 (2.35 s.d.)	0.998 (2.91 s.d.)

TABLE II: Expected and observed CL_{H_x} and $1 - CL_s$ values for $J^P = 0^-$ and $J^P = 2^+$ VX associated production, assuming signal cross sections equal to the 125 GeV SM Higgs production cross section multiplied by $\mu = 1.23$. The null hypothesis is taken to be the sum of the SM Higgs boson signal and background production.

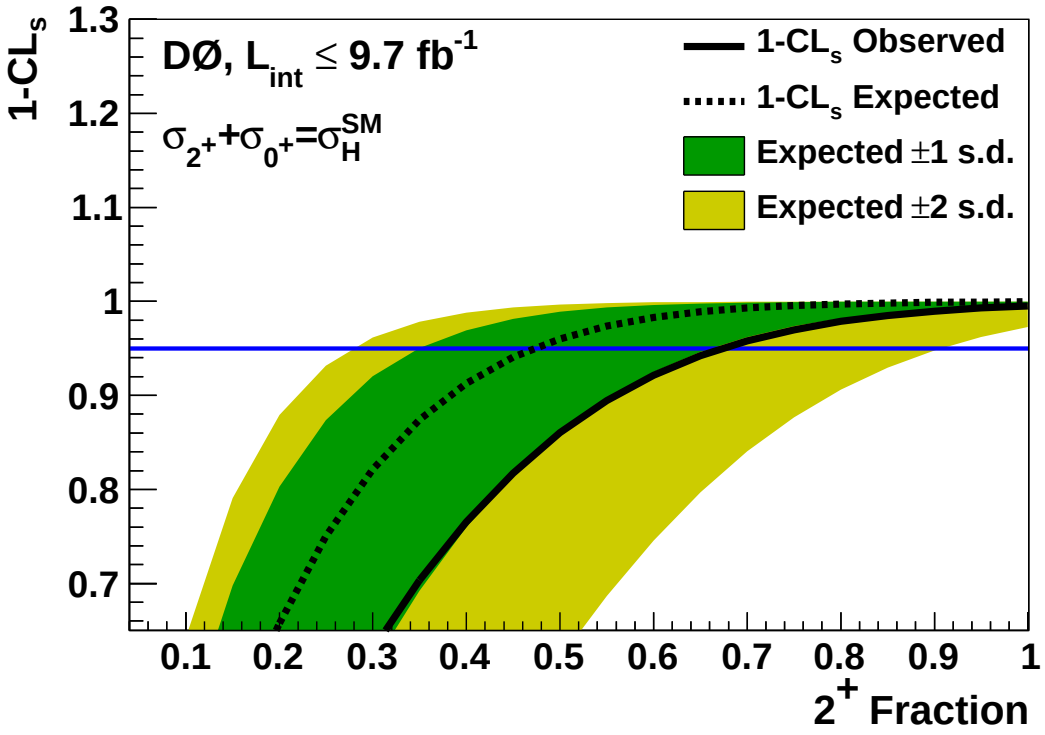

FIG. 8: (color online) $1 - CL_s$ as a function of the $J^P = 2^+$ signal fraction f_{2^+} for $\mu = 1.0$ for all analyses combined. The horizontal solid line corresponds to the 95% CL exclusion. The dark and light shaded regions represent the expected 1 and 2 s.d. fluctuations of the $J^P = 0^+$ hypothesis.

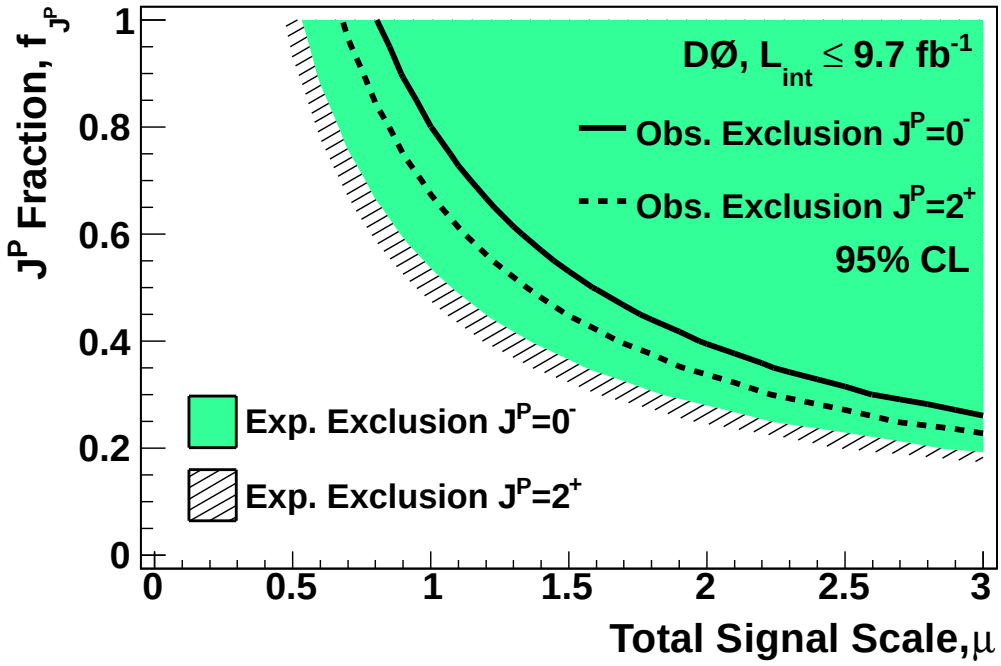

FIG. 9: (color online) The expected 95% CL exclusion (shaded area) and observed 95% CL exclusion (solid line) as functions of the $J^P = 0^-$ signal fraction f_{0^-} and the total signal strength in units of the SM Higgs cross section multiplied by the branching ratio. As functions of the $J^P = 2^+$ signal fraction f_{2^+} and the total signal strength, the expected and observed exclusions are shown as the hatched area and dashed line, respectively.